Computers and Concrete, *Vol. 21, No. 4 (2018) 355-365*
DOI: https://doi.org/10.12989/cac.2018.21.4.355

Direct displacement-based seismic assessment of concrete frames

Chu Peng[1a] and Serhan Guner[*2]

[1]*Department of Civil Engineering, South China University of Technology, 381 Wushan Road, Tianhe District, Guangzhou, 510641, P. R. China*
[2]*Department of Civil and Environmental Engineering, University of Toledo, 2801 W Bancroft St. MS 307, Toledo, Ohio 43606, USA*

(Received July 23, 2017, Revised October 12, 2017, Accepted November 15, 2017)

Abstract. Five previously-tested reinforced concrete frames were modelled using a nonlinear finite element analysis procedure to demonstrate the accurate response simulations for seismically-deficient frames through pushover analyses. The load capacities, story drifts, and failure modes were simulated. This procedure accounts for the effects of shear failures and the shear-axial force interaction, and thus is suitable for modeling seismically-deficient frames. It is demonstrated that a comprehensive analysis method with a capability of simulating material constitutive response and significant second-order mechanisms is essential in achieving a satisfactory response simulation. It is further shown that such analysis methods are invaluable in determining the expected seismic response, safety, and failure mode of the frame structures for a performance-based seismic evaluation. In addition, a new computer program was developed to aid researchers and engineers in the direct displacement-based seismic design process by assessing whether a frame structure meets the code-based performance requirements by analyzing the analysis results. As such, the proposed procedure facilitates the performance-based design of new buildings as well as the numerical assessment and retrofit design of existing buildings. A sample frame analysis was presented to demonstrate the application and verification of the approach.

Keywords: computational mechanics; computer modeling; seismic evaluation of existing buildings; software development & applications; structural safety

1. Introduction

The performance-based seismic design (PBSD) methodologies have found more prevalent use in the seismic design of buildings due to the fact that they consider not only the building performance requirements, but also the economic losses resulting from an earthquake. The PBSD incorporates four specific analysis methods: the linear static analysis, the linear dynamic analysis, the pushover analysis (also called the nonlinear static analysis) and the nonlinear dynamic analysis. The pushover analysis is more accurate than the linear analysis, while being much faster than the nonlinear dynamic analysis-a good compromise for the seismic performance evaluation of building structures.

In the nonlinear pushover analysis of frame structures, one-dimensional distributed nonlinearity fiber elements employing various constitutive relationships represent the most common approach because of their computational efficiency and analytical accuracy. Although several procedures have been proposed, only a small number of them can account for the effects of cyclic loading and shear-axial force interaction, both of which are essential for the seismic performance assessment of frames. Among them are the formulations proposed by Petrangeli *et al*. (1999), Marini and Spacone (2006), Bairan and Mari (2007), Ceresa *et al*. (2009), Guner and Vecchio (2010a, b), and Ferreira *et al*. (2015). For the performance-based earthquake engineering, a computational tool in the form of computer software is required for the application of the formulations. The available tools include SAP2000 (CSI 2013), Ruaumoko (Carr 2007), OpenSees (McKenna *et al*. 2000), Seismostruct (Seismosoft 2014), and VecTor5 (Guner and Vecchio 2008). SAP2000 and Ruaumoko are based on a lumped-plasticity approach, and requires the input of the complete shear response of each plastic hinge. Seismostruct does not have a built-in capability to consider shear effects in a cyclic load analysis of concrete frames. OpenSees does not have pre- and post-processing software for practical applications to aid in the model creation and result visualization such as crack patterns, deformed shape, and failure modes. Consequently, the program VecTor5 is used in this current study.

VecTor5 is a fiber-based, distributed-plasticity finite element modeling procedure for shear-critical planar frames. It was previously verified for the static (monotonic and cyclic) and dynamic (impact, blast and earthquake) load conditions (Guner and Vecchio 2010a, 2010b, 2011, 2012, and Guner 2016), and found to accurately simulate experimental response of frames including strengths, stiffnesses, ductilities and failure modes under these load conditions. Parameters such as crack widths, reinforcement strains and member deformations were also simulated well. This current study is aimed at further verifying this procedure's accuracy and applicability in seismic performance evaluation by using pushover analyses. This

∗Corresponding author, Assistant Professor
E-mail: serhan.guner@utoledo.edu
[a]Undergraduate Student
E-mail: peng.chu@mail.scut.edu.cn

ISSN: 1598-8198 (Print), 1598-818X (Online)

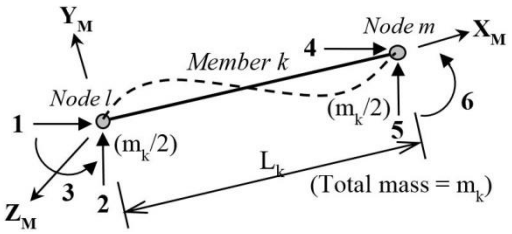

(a) Frame element

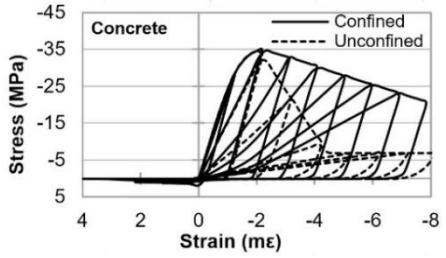

(b) Concrete hysteresis

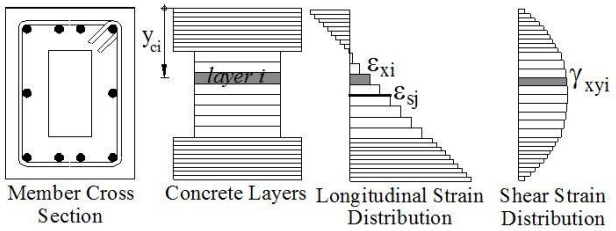

(c) Layered section approach

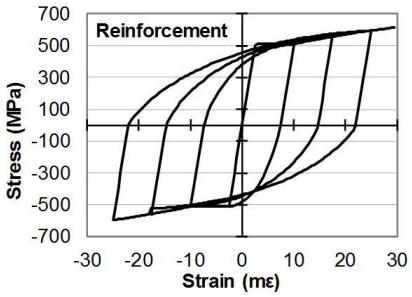

(d) Reinforcement hysteresis

Fig. 1 Finite element modeling technique employed

study also introduces a practical computer program for the direct displacement-based seismic design verification of concrete frames, which uses the analysis output from the pushover analysis. The application of this program is also presented.

2. Research significance

Accurate seismic performance assessment of frame structures is of vital importance in seismic design. The nonlinear finite element analysis procedures are valuable tools in performing a pushover analysis to aid the performance-based seismic design. However, the number of available computer programs with a capability to simulate the axial and shear force interactions is limited. An existing analysis program is used in this study to verify its accuracy and demonstrate its applicability in seismic performance evaluation through pushover analyses. This program uses default analysis options and material models without requiring any calibration or pre-analysis calculations to simulate the shear response of beams and columns. Furthermore, the available nonlinear analysis programs do not directly correlate the analysis results with the various performance objectives identified in seismic building codes. To aid with this process, a practice-oriented computer code and associated program is developed to directly determine whether the frame analyzed meets the performance objective selected by the structure owners, which is identified in the current seismic design codes.

3. Finite element modeling procedure

The analysis procedure employed uses six-degree-of-freedom linear elements, as shown in Fig. 1(a), within a distributed-plasticity frame analysis algorithm using an iterative, total-load, secant-stiffness formulation. The nonlinear sectional analysis algorithms provide a comprehensive and accurate representation of the concrete response, including the shear effects coupled with axial and flexural responses, based on the Disturbed Stress Field Model (Vecchio 2000). A fiber discretization of the cross-section is employed as illustrated in Fig. 1(c). Each concrete and longitudinal reinforcing bar layers are defined as discrete elements while the transverse and out-of-plane reinforcement is smeared within the concrete layers. The out-of-plane reinforcement provides confinement to concrete layers. The main sectional compatibility requirement is that “plane sections remain plane”, while the sectional equilibrium requirements include balancing the axial force, shear force, and bending moment (calculated by the global frame analysis). A parabolic shear strain distribution through the section depth is assumed. To compensate for the clamping stresses in the transverse direction (assumed to be zero), a shear protection algorithm is developed to prevent premature failures of D-regions. The procedure is capable of considering such second-order effects as material and geometric nonlinearities, compression softening due to transverse cracking, tension stiffening due to load transfer between cracked concrete and reinforcement, tension softening due to fracture-related mechanisms, confined strength, shear slip along crack surfaces, concrete prestrains, reinforcement dowel action, and reinforcement buckling.

The numerical models were created using the published specimen details (e.g., the geometry, support conditions, cross-section details, concrete strengths, and reinforcement grades) with the help of a pre-processor program FormWorks Plus (Sadeghian 2012, Blosser and Guner 2016). The default models were used for the material modeling throughout this study (see Table 1). The out-of-plane confinement reinforcement due to closed stirrups and ties was assigned into the core concrete layers. The results investigated included the load-deflection responses, story drifts, concrete crack widths, reinforcement stresses and strains, the failure modes, and the failure displacement. The analysis results were visually verified through the graphical post-processor program Janus (Chak 2013, Loya *et al.* 2015).

Table 1 Default material behavior models used

Concrete Behavior	Model	Reinforcement Behavior	Model
Compression Pre-Peak	Hognestad Parabola	Hysteresis	Seckin / Bauschinger
Compression Post-Peak	Modified Park-Kent	Dowel Action	Tassios (Crack Slip)
Compression Softening	Vecchio 1992-A	Buckling	Refined Dhakal-Maekawa
Tension Stiffening	Modified Bentz 2003		
Tension Softening	Considered	**Analysis Options**	**Model**
Confined Strength	Kupfer/Richard	Geometric Nonlinearity	Considered
Dilatation	Variable Kupfer	Shear Analysis Mode	Parabolic Shear Strain
Cracking Criterion	Mohr-Coulomb	Shear Protection	On
Crack Width Check	Limit=Agg/5	Convergence Limit	1.00001
Hysteresis	Nonlinear (Vecchio)	Maximum No of Iterations	100
Slip Distortion	Vecchio-Lai		

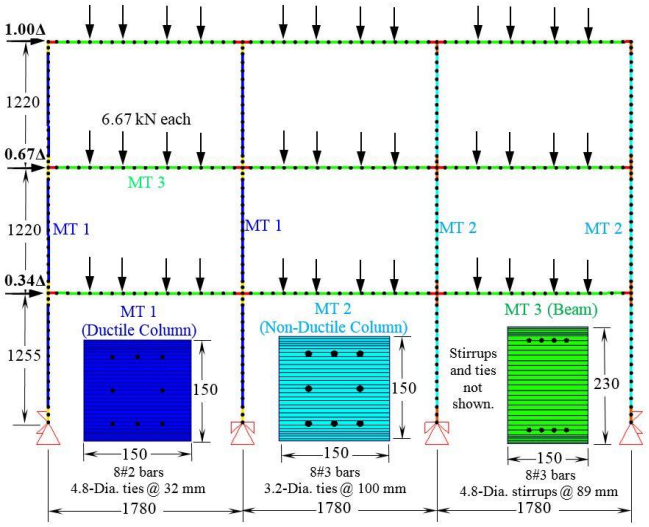

Fig. 2 Finite element model of Ghannoum-Moehle frame (as shown by post-processor Janus)

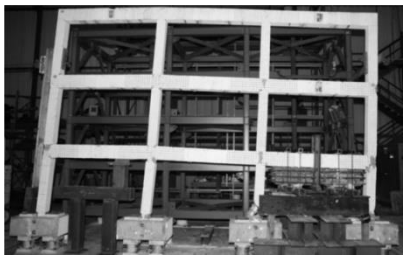

(a) Experiment failure mode (Ghannoum and Moehle, 2012)

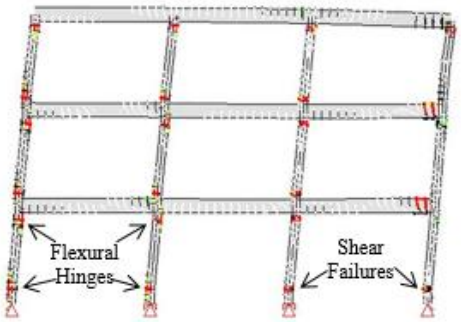

(b) Analysis (as shown by post-processor Janus)

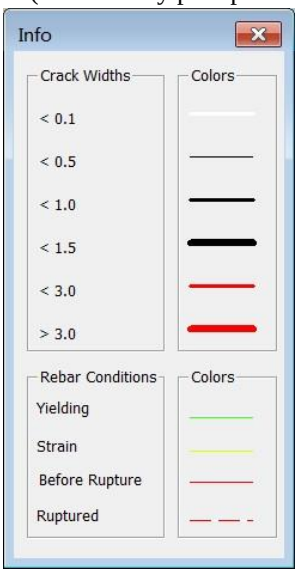

(c) Crack and rebar legend from Janus

Fig. 3 Comparison of experiment and analysis failure mode

4. Finite element modelling of RC frames

4.1 Ghannoum and Moehle frame

A 1/3-scale, three-bay, three-story, planar reinforced concrete frame was tested by Ghannoum and Moehle (2012). Two columns had ductile design details with small stirrup spacing, satisfying the ACI 318-08 (2008) requirements for special moment-resisting frames, while the other two columns had older-type, non-ductile design details. The frame was tested on a shake table subjected to the 1985 Chile earthquake with a scale factor of $1/\sqrt{3}$.

The frame was modelled using 349 nodes and 354 members. Three member types were used for the columns and beams; three additional member types were used to model the beam-column joints. The default analysis options and material behaviour models were used with no adjustments made. The lead weight blocks were modelled using point loads, and the pushover loading was applied in a displacement-controlled mode with the proportions shown in Fig. 2.

The analytical base shear versus story drift response is compared with the experimental backbone curve in Fig. 4(a). The analysis captured the experimental load capacity reasonably well. The slight underestimation may have resulted from the idealized pushover load distribution or other factors such as the post-tensioned restraining system or lead weights bolted to the beams, both of which were not explicitly modelled in the analysis.

The experimental failure mode involved shear failures of the non-ductile columns at their bases which were successfully captured in the analysis (see Fig. 3). For the ductile columns, both experiment and analytical results

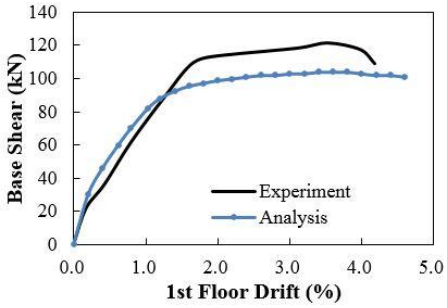

(a) Ghannoum-Moehle frame

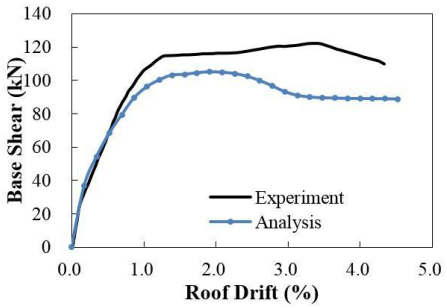

(b) Wu *et al*. frame

Fig. 4 Comparison of experiment and analysis results

indicated the formation of significant plastic hinges, resulting in large rotation near beam-column joints and the supports.

4.2 Wu et al. frame

A single-story, four-column, 1/3-scale planar frame with two ductile and two non-ductile columns was tested by Wu *et al.* (2008). The frame was loaded with lead packet stacks, weighing 173.6 kN in total, to represent the weight and mass associated with higher floors. The earthquake loading was applied through a shake table.

The frame was modelled using the experimental details, and analyzed using a pushover analysis as shown in Fig. 5. Fig. 4(b) shows the calculated and observed base shear versus roof drift responses. The analysis was able to capture the load capacity of the frame with predicted-to-observed ratio of 0.86. The stiffness degradation was also captured well.

The ductile columns experienced a flexural failure with significant plastic deformations during the experiment, which was simulated well in the analysis. The nonductile columns experienced axial and shear failure in the experiment. The column members near beam-column joints showed shear and axial failures in the analysis, confirming suitability of the numerical simulation procedure in capturing the failure mode (see Fig. 6).

4.3 Yavari el al. frame

Two 1/2.25-scale, two-bay, two-story reinforced concrete frame specimens were tested by Yavari *et al*. (2013), as shown in Fig. 7. These two specimens are denoted as MCFS (moderate axial load, confined joints, flexure-shear failure type), HCFS (high axial load, confined joints, flexure-shear failure type). Two steel frames were bolted to the shaking table on either side of the specimens to brace the specimens in the out-of-plane direction by means of machined rollers at each beam level. Both of the

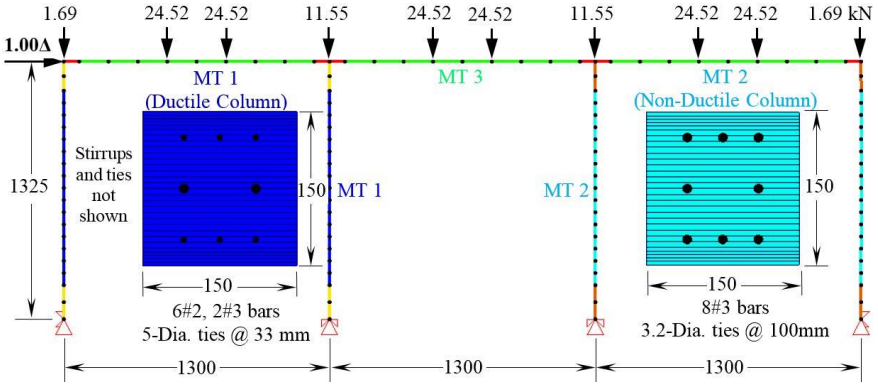

Fig. 5 Finite element model of Wu *et al*. frame (as shown by post-processor Janus)

Ductile Column Non-ductile Column

(a) Experiment (Wu *et al*. 2008)

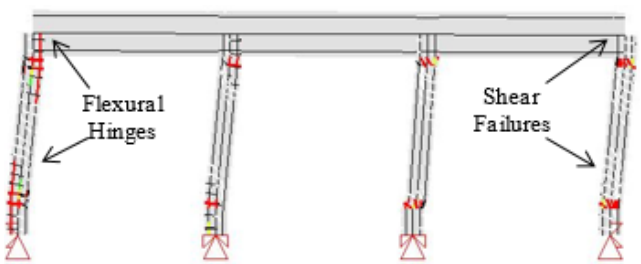

(b) Analysis (as shown by post-processor Janus)

Fig. 6 Comparison of experiment and analysis failure mode of Wu *et al.* frame

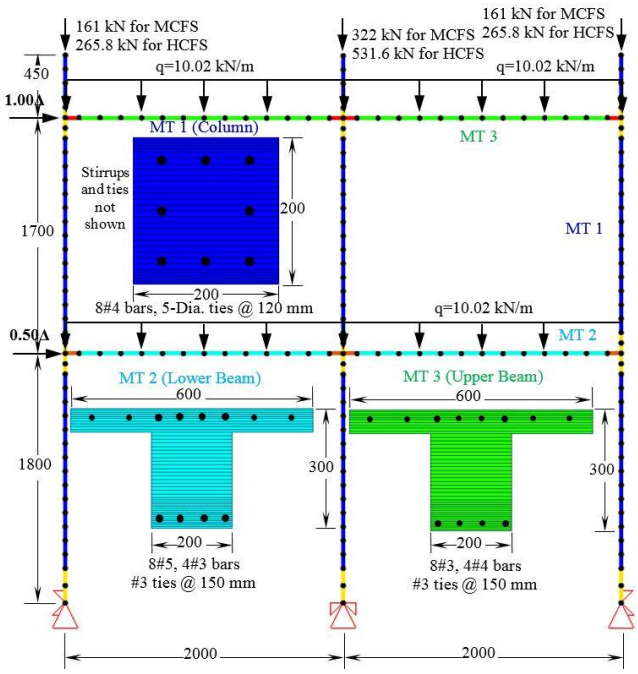

Fig. 7 Finite element model of Yavari *et al*. frame (as shown by post-processor Janus)

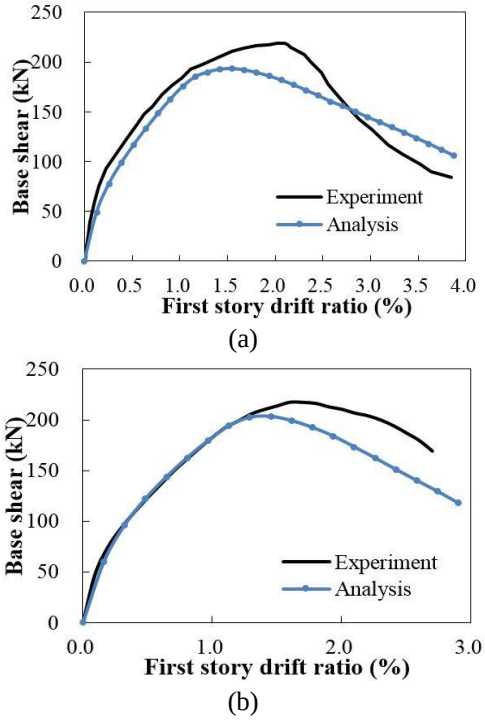

(a)

(b)

Fig. 8 Comparison of experiment and analysis results

test frames were subjected to the same shake table motion recorded from the 1999 Chi-Chi earthquake.

The frames were modelled using a similar approach as discussed previously and analyzed subjected to pushover loading, as shown in Fig. 7. As seen in Fig. 8, the analytical and experiment results are quite similar in terms of peak loads. Yavari *et al*. (2013) defines the shear failure as 20% reduction in the shear resistance, accompanied by diagonal cracking. Based on this criterion, for the MCFS specimen,

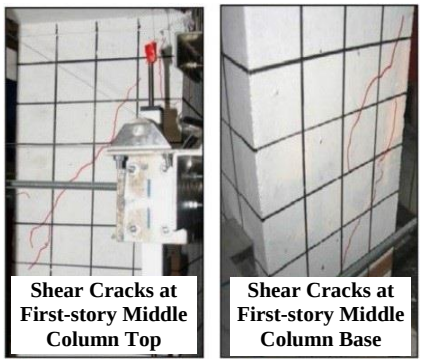

(a) Experiment (Yavari *et al*. 2013)

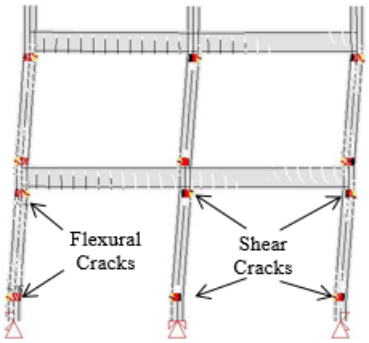

(b) Analysis (as shown by post-processor)

Fig. 9 Comparison of experiment and analysis failure mode of MCFS

(a) Experiment (Yavari *et al*. 2013)

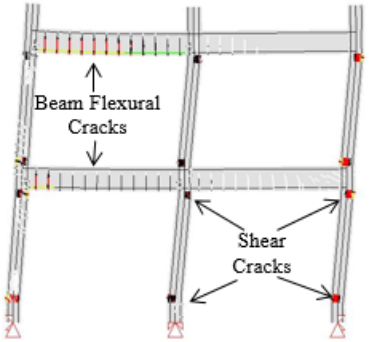

(b) Analysis (as shown by post-processor)

Fig. 10 Comparison of experiment and analysis failure mode of HCFS

the experimental failure mode involved a flexural-shear-axial failure. The middle column first showed flexural cracks, then a shear failure occurred, followed by an axial

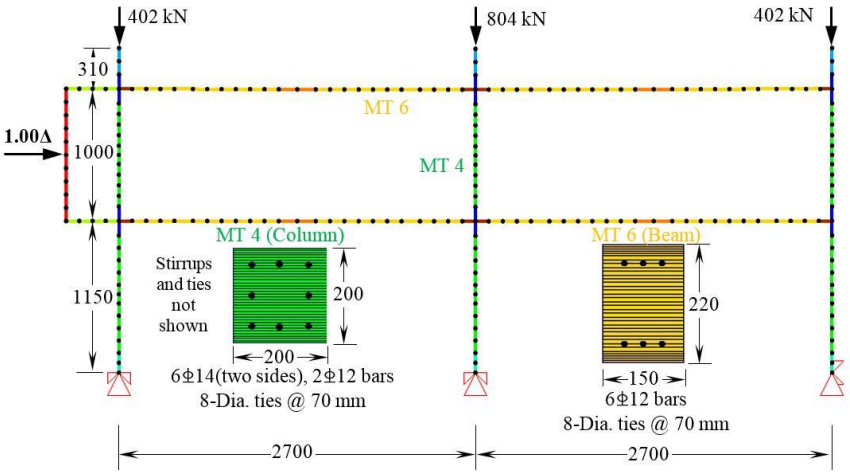

Fig. 11 Finite element model of Xue *et al.* frame (as shown by post-processor Janus)

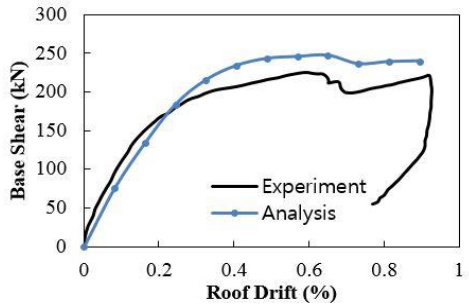

Fig. 12 Comparison of experiment and analysis results of Xue *et al*. frame

failure. Afterwards, the two side columns showed flexural and shear failures. The analysis also showed significant flexural cracks, and exhibited a shear failure with the base shear capacity dropped more than 20%. Fig. 9(b) shows the diagonal shear cracks successfully captured in the analysis. Consequently, the calculated failure mode matches well with the experiment failure mode.

For the HCFS specimen, the experimental failure mode involved a flexural-shear-axial failure. Due to the high axial load on the middle column, an axial failure occurred immediately after the shear failure. The failure mode of analysis was the same as the experimental failure mode, as shown in Fig. 10. First, the frame sustained significant flexural cracks followed by the formation of the plastic hinges at the column ends. Afterwards, the members at the column bases exhibited shear failures. The beams in the left span had more cracks compared to the MCFS specimen, possibly due to the high axial load on the middle column.

4.4 Xue et al. frame

A 1/5-scale, two-bay, two-story, high performance concrete frame was tested by Xue *et al.* (2011). It was designed in conformity with the requirement of ACI 318-08 (2008), and tested under reversed-cyclic displacement excursions. Three constant column axial loads were added to simulate the gravity load coming from the upper stories. The lateral force was applied using a displacement-controlled loading protocol at the mid-point between the

(a) Experiment (Xue *et al*. 2011)

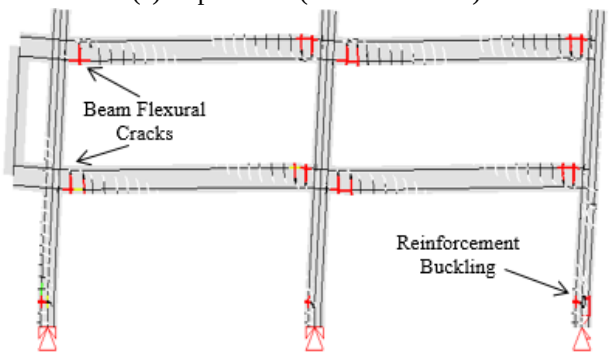

(b) Analysis (as shown by Janus)

Fig. 13 Comparison of experiment and analysis failure modes for the Xue *et al.* frame

first and second story beams.

The frame was modelled using the program VecTor5. The supports at the lower ends of each column were modelled as fixed. A displacement-controlled pushover analysis was performed to obtain the backbone response curve.

As shown in Fig. 12, the analysis captured the loading capacity and the failure drift very well, with a predicted-to-observed ratio of 1.10 and 0.98, respectively.

The frame exhibited a partial beam-sidesway mechanisms in the experiment. The formation of plastic hinges at the column bases led to the failure of the frame. The analysis captured the experimental failure mode, as shown in Fig. 13. In the analysis, the longitudinal reinforcements in beam ends reached their yield strength and formed plastic hinges. The frame failed due to the longitudinal reinforcement buckling at the right column base.

Table 2 Comparison of experiment and analyses results of five frames

Frame	Peak load (kN)			Peak drift* (%)		
	Analysis	Experiment	Ratio	Analysis	Experiment	Ratio
Ghannoum	105	122	0.86	4.60	4.18	1.10
Wu	107	124	0.86	4.52	4.37	1.03
MCFS	195	220	0.89	3.89	3.86	1.01
HCFS	205	218	0.94	2.89	2.71	1.07
Xue	249	227	1.10	0.90	0.92	0.98
		Mean	0.93		Mean	1.04
		COV (%)	10.7		COV (%)	4.6

*Peak drift: drift at frame failure

4.5 Summary of results

The experiment and analysis results of all of the five frames are summarized in Table 2, which indicates that the numerical procedure provides satisfactory accuracy in both the load capacity and interstory drift ratio. The ratio of the predicted-to-observed peak load for all five frames has a mean of 0.93 with a coefficient of covariation (COV) of 10.7%. The failure drift ratio was predicted with a mean value of 1.04 and a COV of 4.6%. These values are well within the accuracy margins that can be expected from the nonlinear analysis of concrete frames subjected to their ultimate collapse conditions. The minor underestimation in the peak load capacities of four of the frames can be attributed to several factors including variability in the material properties and workmanship, challenges in modelling the exact experimental boundary conditions, and how the forces are measured during the experimental program. The slight overestimation in the peak load capacity of the Xue frame is attributed to the simplified (i.e., rigidly-connected) modeling of the steel load application column used in the experimental program. The analyses were conducted using a laptop computer with a processor of Intel Core i5-4210M @ 2.60 GHz, RAM of 4.00 GB, and a solid-state drive speed of 200 MB/s. The longest analysis required a computational time of 9 minutes and 32 seconds for the Ghannoum-Moehle frame.

5. Overview of the program DDBSD

Priestley (1993, 1998), Priestley and Kowalsky (2000) and Priestley *et al*. (2007) pioneered the direct displacement-based seismic design method. The accuracy of this approach was verified by analyzing a series of structures with different structural types and materials using inelastic-time-history analyses. Extensive design examples using this approach were demonstrated in Priestley *et al*. (2007) to illustrate the reliability of this approach. A program named DDBSD (Direct Displacement-Based Seismic Design) was developed to utilize the nonlinear finite element analysis output and the response spectrum in ASCE 7-10 (2013) code to verify whether the performance

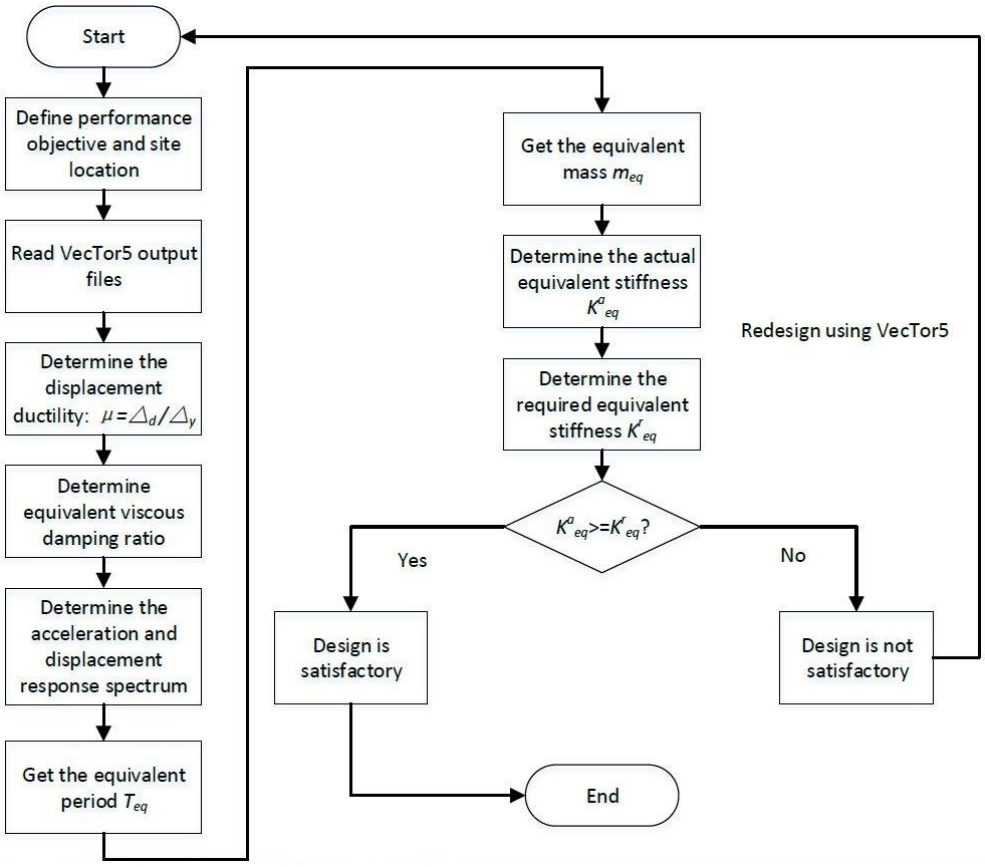

Fig. 14 Flowchart of the DDBSD program

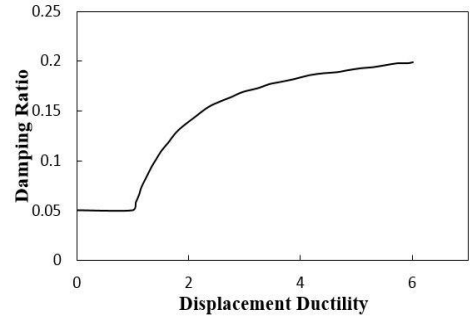

(a) Damping ratio (Priestley *et al*. 2007)

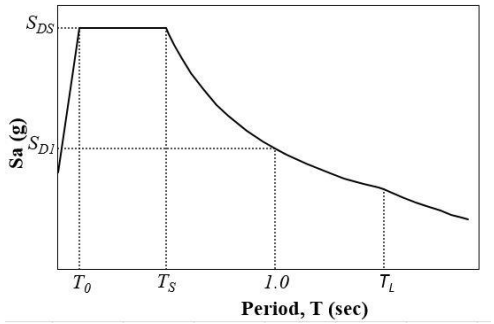

(b) Acceleration response spectrum (ASCE 7-10 2013)

Fig. 15 Explanation of the parameters used in DDBSD program

objectives in FEMA 356 (2000) is satisfied or not for a given frame structure using the direct displacement-based seismic design method. Although this program is specially written for the finite element analysis program VecTor5, the proposed methodology can be applied to any other nonlinear finite element procedure.

The flowchart of the program DDBSD is presented in Fig. 14. The program will first require the users to select performance objectives of the structure to resist earthquake (i.e., limited objective, basic safety objective, enhanced objective). Then the program will read the analysis output files to obtain the yield displacement Δ_y value. The design displacement Δ_d value is then calculated using the drift limit ratio recommended by FEMA 356 (2000) times the structure height. The ratio of the design displacement to the yield displacement gives the displacement ductility. Using the displacement ductility, an equivalent viscous damping ratio is obtained using Fig. 15(a). The design acceleration response spectrum is then constructed using the user-given parameters T_L, S_S and S_1, these parameters can be calculated through the U.S. Seismic Design Maps (2016) by using the structure location and the site soil classification. After a series of calculations, the design displacement response spectrum is obtained, through which the equivalent period T_{eq} is obtained. Using the equivalent period T_{eq} and the equivalent mass m_{eq}, the required equivalent stiffness K^r_{eq} is obtained. The actual equivalent stiffness K^a_{eq} is obtained using the load-displacement response of the pushover analysis. By comparing K^r_{eq} and K^a_{eq}, a decision can be made regarding whether or not the structure analyzed can satisfy the performance objectives of the FEMA 356 (2000) code, which are related to the performance levels (i.e., immediate occupancy, life safety and collapse prevention) and the earthquake hazard levels.

The design displacement response spectrum is obtained from the design acceleration response spectrum shown in Fig. 15(b), using Eqs. (1)-(3) from Filiatrault and Folz (2002).

$$S_{DCode} = \frac{T^2}{4\pi^2} S_{ACode} \tag{1}$$

$$S_{D\varsigma eq} = \sqrt{\frac{0.07}{0.02 + \varsigma_{eq}}} S_{DCode} \tag{2}$$

$$S_{DTr} = \left(T_r / 474\right)^{0.44} S_{DCode} \tag{3}$$

Eq. (1) is used to convert the code design acceleration response spectrum S_{ACode} for a given seismic zone into a corresponding displacement response spectrum S_{DCode}. Eq. (2) is used when the viscous damping ratio is different from 5%. Eq. (3) is used when the mean return period T_r is different from 474 years. T_r is related to the earthquake hazard levels. Based on FEMA 356 (2000) recommendation, T_r is 72, 225, 474, 2,475 years for 50%, 20%, 10% and 2% probability of exceedance in fifty years, respectively.

The program DDBSD calculates the required equivalent stiffness using Eq. (4) from Priestley *et al*. (2007).

$$K^r_{eq} = \frac{4\pi^2 m_{eq}}{T^2_{eq}} \tag{4}$$

T_{eq} is the equivalent period and m_{eq} is the equivalent mass. The equivalent period is obtained from the design displacement response spectrum, using the design displacement as the vertical coordinate.

The equivalent mass represents the mass of the equivalent one-degree-of-freedom system, and calculated using Eq. (5) from Priestley *et al*. (2007).

$$m_{eq} = \sum_{i=1}^{n} \frac{m_i \Delta_i}{\Delta_d} \tag{5}$$

Actual equivalent stiffness is the value of the design base shear divided by the design displacement. The design base shear is obtained from the nonlinear pushover analysis results.

By comparing the required equivalent stiffness and the actual equivalent stiffness, the program checks whether the structure analyzed satisfies the performance objectives of the FEMA 356 (2000) code. If the actual equivalent stiffness is greater than or equal to the required equivalent stiffness, the program indicates that the structure achieves the required performance objective.

6. Direct displacement-based seismic design example

To demonstrate the application of the DDBSD program, the analysis results of the Wu *et al*. frame was used. It was assumed that the frame is located in Los Angeles, USA, and constructed in a soil-type D (i.e., stiff soil). The seismic design check was performed for the basic safety objective for demonstration purposes, therefore, the life safety and

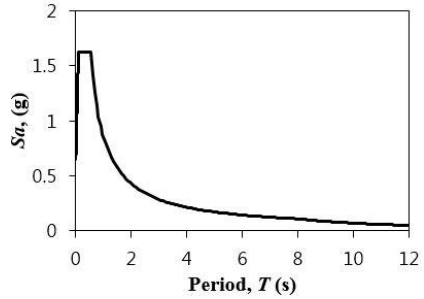

(a) Spectral acceleration in analysis

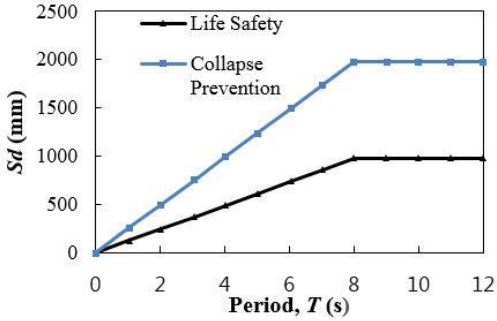

(b) Spectral displacement in analysis

Fig. 16 Response spectrum

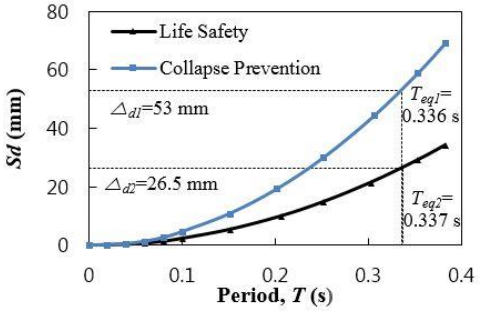

(a) Equivalent periods

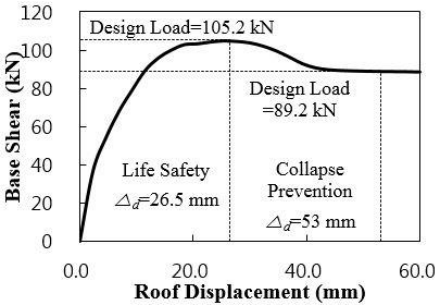

(b) Design Load

Fig. 17 Response spectrum

collapse prevention limit states must be achieved under the earthquake hazard level of 10% and 2% probability of exceedance in 50 years, respectively. According to the performance level drift limit recommendation of FEMA 356 (2000), the design displacement for the life safety limit state is 26.5 mm (2% drift), while it is 53 mm (4% drift) for the collapse prevention limit state.

The DDBSD program first detects the average longitudinal reinforcement stresses using the analysis output, and compares them with the yield stress values to obtain the corresponding yield displacement. For this frame, a yield displacement value of 6 mm was obtained. The ratio of the design displacement to the yield displacement is the displacement ductility, which is 4.4 for the life safety limit state and 8.8 for the collapse prevention limit state. The viscous damping ratios were calculated using Fig. 15(a) to be 18.9% and 20% for the life safety limit and collapse prevention limit states, respectively.

For the structure location and the soil type, the T_L, S_S and S_1 values were obtained using the U.S. Seismic Design Maps (2016) as 8s, 2.433g, and 0.853g, respectively. The program DDBSD uses these parameters to calculate the design acceleration response spectrum per the ASCE 7-10 (2013) code, as shown in Fig. 16(a). For the Wu *et al*. frame to satisfy the basic safety objective, the return period is 474 and 2,475 years for the life safety and collapse prevention limit states, respectively. Using Eqs. (1)-(3), the design displacement response spectrum was obtained as showed in Fig. 16(b).

The equivalent periods T_{ea} for the life safety limit state and the collapse prevention limit state were then obtained using the design displacement response spectrum, as shown in Fig. 17(a). The program DDBSD calculates the total mass using the analysis output files and obtains the equivalent mass m_{eq} using Eq. (5).

Table 3 Summary of the seismic design example

Performance Level	Damping Ratio	T_{ea} (s)	K^r_{ea} (N/mm)	K^a_{ea} (N/mm)	K^a_{ea} / K^r_{eq}
Life Safety	18.9%	0.337	4254.2	3969.8	0.93
Collapse Prevention	20%	0.336	2736.6	1683	0.61

The required equivalent stiffness K^r_{ea} was calculated using Eq. (4), which was found to be 4254.2 and 2736.6 N/mm for the life safety and collapse prevention limit states, respectively. The actual equivalent stiffness K^a_{ea} was then calculated by dividing the design load by the design displacement obtained from the pushover analysis curve. K^a_{ea} was calculated to be 3969.8 and 1683 N/mm for the life safety and collapse prevention limit states.

Table 3 shows the summary of the direct displacement-based seismic design checks performed on the Wu *et al*. frame. Based on the results, the structure can satisfy neither the life safety nor the collapse prevention limit state. The actual equivalent stiffness is 7% smaller than the required equivalent stiffness for the life safety limit state and 39% smaller for the collapse prevention limit state. Therefore, the structure cannot meet the basic safety objective recommended by FEMA 356 (2000) code.

To validate the results obtained by the DDBSD program, a nonlinear static procedure (NSP) prescribed in ASCE 41-13 document was conducted. The NSP is based on the assumption that the response of the MDOF structure can be related to that of an equivalent SDOF. For this purpose, the NSP is a useful tool to the engineering practitioner for the assessment of the seismic behavior of structures. In the NSP procedure, the gravity loads are applied followed by a lateral load pattern that is gradually increased in the direction under consideration. The investigated Wu *et al*. frame was pushed using a single lateral load pattern at the

first story level to achieve the target displacement (δ_t) required. At each load step, the base shear and the corresponding roof displacement can be plotted to create the capacity or pushover curve. Based on the obtained response, it is possible to visualize the maximum base shear that the structure is capable to withstand during the earthquake event. The target displacement was calculated based on the displacement coefficient method defined in ASCE 41-13. This method modifies the elastic response of an equivalent SDOF system with coefficients C_0, C_1 and C_2 as expressed as follows

$$\delta_t = C_0 C_1 C_2 S_a \frac{Te^2}{4\pi^2} g \tag{6}$$

where S_a is the response spectrum acceleration at the effective fundamental vibration period and damping ratio, g is the acceleration of gravity, and T_e is the effective fundamental period of the building in the direction under consideration as computed from:

$$T_e = T_i \sqrt{\frac{K_i}{K_e}} \tag{7}$$

where T_i, K_i, and K_e are the elastic fundamental period, elastic lateral stiffness, and effective lateral stiffness, respectively.

Using Eqs. (6) and (7), the target displacement was calculated to be 80.6 mm, which corresponds to a 6.1% story drift for the collapse prevention limit state. The maximum story drifts recommended by FEMA 356 are 1%, 2% and 4% for the immediate occupancy (IO), life safety (LS), and collapse prevention (CP) limit states, respectively. Consequently, the Wu *et al*. frame does not satisfy any of the performance levels. The ratio of the maximum drift recommended by FEMA 356 to that calculated using the target displacement method is 0.65, whereas the ratio calculated using the DDBSD method is 0.61. The good agreement between the two methods validates the results obtained.

7. Conclusions

This paper verified the accuracy of a nonlinear finite element analysis procedure in seismic performance evaluation by modelling five previously-tested seismically-deficient concrete frame structures, and comparing the simulated load capacities, drift ratios, and the failure modes with the experimental results. A computational program DDBSD was developed to check whether the structure can satisfy the seismic performance requirements of the FEMA 356 (2000) code using the analysis output from the nonlinear finite element analysis procedure, response spectrum relation in ASCE 7-10 (2013) code, and direct displacement-based seismic design methods. In addition, a nonlinear static procedure (NSP) prescribed in ASCE 41-13 was performed to validate the results obtained. An example was presented for the application of the program DDBSD. The results of the investigation indicate the following conclusions.

- The nonlinear finite element analysis procedure used predicted the load, drift and failure responses of the frames examined accurately. The ratio of the predicted-to-observed peak loads for all five frames had a mean of 0.93 with a coefficient of variation (COV) of 10.7 %. The drifts at failure were also predicted well with a mean value of 1.04 and COV of 4.6%.
- The pushover analysis employed consumed a fraction of the analysis times required by nonlinear dynamic analysis procedures, while providing sufficiently accurate simulation of the seismic response of the frames examined.
- Pre- and post-processor software is essential in understanding the behavior and the failure mode of frame structures by showing the sequence of nonlinear events, crack propagation, concrete and reinforcement stresses/strains, and the deflected shapes of the frames.
- Pushover analysis results from the nonlinear finite element analysis procedure can be used for the direct displacement-based seismic design, to aid the determination of whether or not the designed structure can meet the seismic code requirements.
- The program DDBSD can be used by practicing engineers to check whether the building can satisfy the seismic design code requirements by using the results of a nonlinear pushover analysis. The presented methodology has a general applicability to other nonlinear finite element analysis programs.

Acknowledgments

This research is funded by China Scholarship Council and Mitacs Globalink Program. The supports are gratefully acknowledged. The authors would also like to acknowledge the contribution of Salim Khoso and Rafael Salgado, PhD candidates in the Department of Civil Engineering at the University of Toledo, for conducting the nonlinear static procedure as per ASCE 41-13.

References

ACI 318 (2008), Building Code Requirements for Structural Concrete, American Concrete Institute, Farmington Hills, MI, USA.

ASCE 7-10 (2013), Minimum Design Loads for Buildings and Other Structures, American Society of Civil Engineers, Reston, Virginia, USA.

ASCE 41-13 (2013), Seismic Evaluation and Retrofit of Existing Buildings, American Society of Civil Engineers, Reston, Virginia, USA.

Bairan, J.M. and Mari, A.R. (2007), "Multiaxial-coupled analysis of RC cross-sections subjected to combined forces", *Eng. Struct.*, **29**(8), 1722-1738.

Blosser, K. and Guner, S. (2016), *User's Manual of FormWorks plus for VecTor5*, Department of Civil Engineering, University of Toledo, Toledo, USA.

Carr, A.J. (2007), *Ruaumoko Manual: Volume 1*, Computer Program Library, University of Canterbury, Christchurch, New Zealand.

Ceresa, P., Petrini, L., Pinho, R. and Sousa, R. (2009), "A fibre flexure-shear model for seismic analysis of RC-framed

structures", *Earthq. Eng. Struct. Dyn.*, **38**(5), 565-586.
Chak, I.N. (2013), "Janus: a post-processor for VecTor analysis software", M.A.Sc. Dissertation, Department of Civil Engineering, University of Toronto, Toronto, Canada.
CSI (2013), Analysis Reference Manual for SAP2000® , ETABS® and SAFE™, Computers and Structures, Inc., Berkeley, CA, USA.
FEMA 356 (2000), Prestandard and Commentary for the Seismic Rehabilitation of Buildings, Reston, Virginia.
Ferreira, D., Bairán, J.M. and Marí, A. (2015), "Shear strengthening of reinforced concrete beams by means of vertical prestressed reinforcement", *Struct. Infrastr. Eng. Mainten. Manage. Life-C. Des. Perform.*, **12**(3), 394-410.
Filiatrault, A. and Folz, B. (2002), "Performance-based seismic design of wood framed buildings", *J. Struct. Eng.*, **128**(1), 39-47.
Ghannoum, W.M. and Moehle, J.P. (2012), "Shake-table tests of a concrete frame sustaining column axial failures", *ACI Struct. J.*, **109**(3), 393-402.
Guner, S. (2016), "Simplified modeling of frame elements subjected to blast loads", *ACI Struct. J.*, **113**(2), 363-372.
Guner, S. and Vecchio, F.J. (2008), *User's Manual of VecTor5*, Department of Civil Engineering, University of Toronto, Toronto, Canada.
Guner, S. and Vecchio, F.J. (2010a), "Pushover analysis of shear-critical frames: formulation", *ACI Struct. J.*, **107**(1), 63-71.
Guner, S. and Vecchio, F.J. (2010b), "Pushover analysis of shear-critical frames: verification and application", *ACI Struct. J.*, **107**(1), 72-81.
Guner, S. and Vecchio, F.J. (2011), "Analysis of shear-critical reinforced concrete plane frame elements under cyclic loading", *J. Struct. Eng.*, ASCE, **137**(8), 834-843.
Guner, S. and Vecchio, F.J. (2012), "Simplified method for nonlinear dynamic analysis of shear-critical frames", *ACI Struct. J.*, **109**(5), 727-737.
Loya, A.S., Lourenço, D.D.S, Guner, S. and Vecchio, F.J. (2015), *User's Manual of Janus for VecTor5*, Department of Civil Engineering, University of Toledo, Toledo, USA.
Marini, A. and Spacone, E. (2006), "Analysis of reinforced concrete elements including shear effects", *ACI Struct. J.*, **103**(5), 645-655.
McKenna, F., Fenves, G.L., Scott, M.H. and Jeremic, B. (2000), "Open system for earthquake engineering simulation (OpenSees)", Pacific Earthquake Engineering Research Center, Univ. of California, Berkeley, CA, USA.
Petrangeli, M., Pinto, P.E. and Ciampi, V. (1999), "Fiber element for cyclic bending and shear of RC structures. I: theory", *J. Eng. Mech.*, **125**(9), 994-1001.
Priestley, M.J.N. (1993), "Myths and fallacies in earthquake engineering-conflicts between design and reality", *Bull. NZ. Nat. Soc. Earthq. Eng.*, **26**(3), 329-341.
Priestley, M.J.N. (1998), "Brief comments on elastic flexibility of reinforced concrete frames, and significance to seismic design", *Bull. NZ. Nat. Soc. Earthq. Eng.*, **31**(2), 246-259.
Priestley, M.J.N. and Kowalsky, M.J. (2000), "Direct displacement-based design of concrete buildings", *Bull. NZ. Nat. Soc. Earthq. Eng.*, **33**(4), 421-444.
Priestley, M.J.N., Calvi, G.M. and Kowalsky, M.J. (2007), *Direct Displacement Based Design of Structures*, Istituto Universitario di Studi Superiori (IUSS) Press, Pavia, Italy.
Sadeghian, V. (2012), "Formworks-plus: improved pre-processor for Vector analysis software", M.A.Sc. Dissertation, Department of Civil Engineering, University of Toronto, Toronto, Canada.
Seismosoft (2014), *Seismostruct User Manual for Version 7.0*, Seismosoft Ltd, Pavia, Italy.
U.S. Seismic Design Maps (2016), United States Geological Survey (maps), Reston, Virginia, USA.
Vecchio, F.J. (2000), "Disturbed stress field model for reinforced concrete: formulation", *J. Struct. Eng.*, **126**(9), 1070-1077.
Wu, C.L., Kuo, W.W., Yang, Y.S., Hwang, S.J., Elwood, K.J., Loh, C.H. and Moehle, J.P. (2008), "Collapse of a nonductile concrete frame: shaking table tests", *Earthq. Eng. Struct. Dyn.*, **38**(2), 205-224.
Xue, W.C., Cheng, B., Zheng, R.G., Li, L. and Li, J. (2011), "Seismic performance of nonprestressed and prestressed HPC frames under low reversed cyclic loading", *J. Struct. Eng.*, **137**(11), 1254-1262.
Yavari, S., Elwood, K.J., Wu, C.L., Lin, S.H., Hwang, S.J. and Moehle, J.P. (2013), "Shaking table tests on reinforced concrete frames without seismic detailing", *ACI Struct. J.*, **110**(6), 1001-1011.

SF